

# Classification of Mobile Laser Scanning Data with Geometric Features and Cylindrical Neighborhood

Semanur SEYFELI<sup>1,2</sup>, Ali Ozgun OK<sup>2</sup>

<sup>1</sup> Hacettepe University, Graduate School of Science and Engineering, Ankara, Turkey

<sup>2</sup> Hacettepe University, Department of Geomatics Engineering, Ankara, Turkey

ORCID: 0000-0003-4944-6276, ORCID: 0000-0001-6538-9633

`semanur.seyfelihacettepe.edu.tr, ozgunok@hacettepe.edu.tr`

**Abstract.** Mobile laser scanning (MLS) is a favored information source for urban areas because of its capacity to gather quick and dense three-dimensional information, and classification studies of these large point clouds are carried out by enriching the data set collected. This study discusses a method for classifying an MLS point cloud by constructing a local neighborhood relationship with cylindrical neighborhood information and augmenting the dataset with geometric features in the absence of RGB images. Two benchmark datasets, TUM-MLS1 and Toronto-3D, were employed. The Random Forest (RF) classifier, which has been preferred in many researches for MLS classification, was built and assessed on eight classes of benchmark datasets for point-based supervised classification. As a result, we achieved 94.5% overall accuracy with only four geometric features for both datasets. When comparing our findings for dataset of TUM-MLS1 to those of a previous study, we found a 2.4% increase in overall accuracy.

**Keywords:** Mobile Laser Scanning, Feature Extraction, Geometric Feature, Cylindrical Neighborhood

## 1. Introduction

Point clouds have become increasingly important in the creation of land use maps, digital elevation models, and three-dimensional city and landscape models. They can be acquired using RGB-D sensors, Synthetic Aperture Radar (SAR), image-based photogrammetry, or Light Detection and Ranging (LiDAR) (Günen, 2022). LiDAR technology is one of the most widely used approaches in mapping and surveying due to its progressive ability to generate dense and extremely precise 3D point clouds. Thus far, advanced systems such as space laser scanning (SLS), airborne laser scanning (ALS), terrestrial laser scanning (TLS), and mobile laser scanning (MLS) have all been successfully developed.

Mobile laser scanning (MLS) is a critical source of data for urban areas, as the road environment enables the collection of high-density, high-accuracy 3D georeferenced point clouds. In general, an MLS system consists of multiple elements such as imaging,

scanning, positioning, and storage systems that are mounted on a mobile platform such as a vehicle (Zhu et al., 2020), a boat (Vaaja et al., 2013), a train (Lou et al., 2018), a backpack (Kukko et al., 2012), or a robot (Gao et al., 2018). Vehicle-based platforms, in particular, are more prevalent in urban areas, owing to their relative speed in regular traffic. As a result, large datasets can be produced in a single day (Kukko et al., 2012). Due to the high density of 3D point clouds generated by MLS systems, it is necessary to develop automated methods for rapid 3D mapping. Numerous approaches have been developed for segment-based and point-based classification of MLS point clouds; however, the problem remains unsolved.

Establishing local neighborhood relationships is the fundamental basis for feature extraction in point-based classification of a point cloud, and various methods can be used to collect local neighborhood information from a point cloud (Wang et al., 2018). The most frequently used in the literature are the spherical neighborhood (Brodu and Lague, 2012) or cylindrical neighborhood (Filin and Pfeifer, 2005) defined by a radius parameter and the k-nearest neighborhood defined by the number of nearest points (Weinmann et al., 2013). Geometric and shape-based properties can be obtained by establishing the neighborhood relationship between the points. As a result, geometric properties such as the size, roughness, and density of a point (or segment) are defined. Shape characteristics are determined by eigenvalues  $\lambda_i$  with  $i=1,2,3$ . A 3x3 covariance matrix is constructed for each point in the neighborhood, and the eigenvalues derived from the covariance matrix are retrieved (Guan et al., 2016). The eigenvalues correspond to the principal axes of the three-dimensional ellipsoid and serve as a shape indicator in point cloud classification. The following are some of the shape properties: linearity, planarity, sphericity, eigentropy, and the sum of the eigenvalues. For the classification phase, various classification approaches including machine learning and deep learning algorithms have been tested.

Zheng et al. (2017) published a study in which they classified MLS point clouds by incorporating geometric properties extracted from cylindrical neighborhoods in addition to point density values. Weinmann (2015) compared the classification performance of 21 geometric 3D and 2D features extracted using the k-nearest neighbors of a given point as neighborhood definitions. Thomas et al. (2018) assessed covariance-based features and color characteristics (if any) across multiple datasets. Atik et al. (2021) evaluated the classification performance of several machine learning methods across a range of scales. For each point, areas with different radii were created using spherical neighborhood, and 13 features derived from the covariance matrix were calculated, including height, roughness, normal change rate, and volume density. Additionally, there are strategies in the literature for identifying points in a point cloud using neighborhood size selection criteria and feature extraction techniques. Demantké et al. (2012) calculated dimension-based features using cylindrical neighborhoods, varying the radius of the neighborhood to determine the optimal radius. Thomas et al. (2018) focused on semantic classification by extracting geometric features using a multi-scale spherical neighborhood strategy. The scale choice was critical because it affects the computation time required to extract geometric features. Wang et al. (2018) utilized supervised classification to evaluate various neighborhood types, including the spherical neighborhood with a fixed radius, the vertical cylindrical neighborhood, the k-nearest neighborhood, and the optimal k-nearest neighborhood, the latter of which used eigenentropy-based scale selection to determine the k value. Günen (2022) described and evaluated the omnivariance-based adaptive feature selection method. The results were also compared to other methods for

determining neighborhood size, such as eigentropy-based neighborhood size selection and a fixed number of  $k$ -nearest neighbors.

The purpose of this study is to implement point-based classification of dense point cloud data collected by a mobile mapping system in urban areas using geometric feature information extracted from cylindrical neighborhood relations. The classification process for MLS point clouds is divided into three stages: (i) establishing local neighborhood relationships, (ii) feature extraction, and (iii) classification. The methodology is validated in this context using benchmark datasets, TUM-MLS1 and Toronto-3D, obtained via vehicle-based MLS systems. These MLS datasets, which each contain eight classes, are evaluated using the Random Forest (Breiman, 2001) approach. The MLS point cloud classification workflow over the local cylindrical neighborhood is depicted in Fig.1.

The main contribution of this article is the presentation of a point-based classification approach for urban outdoor MLS point clouds by extracting the easily accessible geometric features via a local cylindrical neighborhood in the lack of further point information. The rest of the paper was organized as follows: Section 2 defines the methodology, Section 3 describes the dataset and experiments, Section 4 presents the experimental results, and Section 5 includes a summary of our findings.

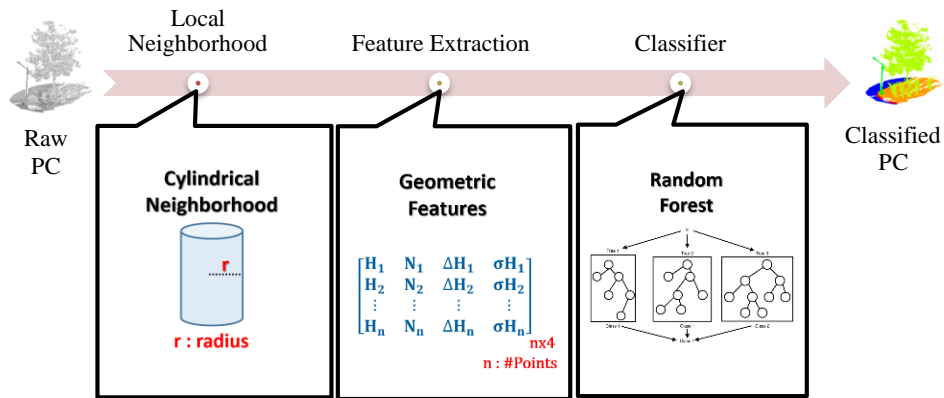


**Fig. 1.** MLS point cloud classification workflow through local cylindrical neighborhood ( $H_n$ ,  $N_n$ ,  $\Delta H_n$ ,  $\sigma H_n$ , denote features extracted for  $n^{\text{th}}$  point (i.e. normalized height, number of points, height difference, and the standard deviation).

## 2. Methodology

Due to the lack of attributes in MLS point clouds; they can be augmented by deriving features from neighborhood relationships between points in a local context or by utilizing RGB images. When RGB images are not available, one of the critical stages of classification is feature extraction for each point (Weinmann, 2015). Because the features will be extracted based on the local neighborhood, it is necessary to determine the neighboring points. The cylindrical neighborhood is a technique for extracting local neighborhood information from a point cloud. The cylindrical neighborhood type is created primarily by specifying a radius. The method's initial stage is to project the point cloud onto a two-dimensional horizontal plane (Fig. 2). Following that, each point in the

point cloud is used as the center, and the points remaining in the circle within the radius determined are searched in two dimensions using the k-d tree algorithm (Bentley, 1975).

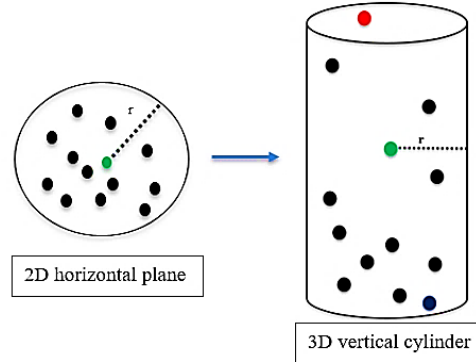


**Fig. 2.** The vertical cylindrical neighborhood of radius  $r$ , and hence the radius  $r$  of the point cloud in the XY plane, is represented (Green: point under consideration, Red: highest point, Blue: lowest point).

To enhance the properties of points, the three-dimensional coordinates of the points within the local vertical cylindrical neighborhood are required during the geometric feature extraction process. Each point in the MLS point cloud is defined by its elevation above the reference surface (e.g. ellipsoid height). By using the Cloth Simulation Filtering (CSF) component of the Cloud Comparing software (Zhang et al., 2016), the elevation of each point was normalized ( $|Z|$ ) according to the terrain height in this study. The first geometric property is a point's normalized height. The height difference ( $\Delta H$ ), defined as the difference between the heights of the maximum and minimum points in the local neighborhood, and the standard deviation ( $\sigma H$ ) of the heights of the points in the local neighborhood, are calculated using the normalized heights obtained. The number of points within the neighborhood ( $N$ ) is another geometric feature. The geometrical features described in the study are listed in Table 1.

**Table 1.** Local geometric features calculated and assigned to each point based on the X, Y, and Z coordinates of the points in the point cloud.

#	Feature	Symbol	Formula
1	normalized height of a point	H	$ Z $
2	number of points in the neighborhood	N	-
3	height difference	$\Delta H$	$h_{\max} - h_{\min}$
4	standard deviation of height	$\sigma H$	$\sqrt{\frac{1}{k} \sum_{j=1}^k (H_j - \mu H)^2}$

The enriched feature set is given as input to the classifier. Random Forest (RF) is one of the most frequently used methods for dense point cloud classification. The RF generates multiple decision trees and then combines them to produce a more accurate and stable estimation (Breiman, 2001).

### 3. Dataset and Experiment

Two MLS datasets, TUM-MLS1 and Toronto-3D, over two urban areas were used to assess the relevance of the proposed approach.

The TUM-MLS1 dataset (Zhu et al., 2020), created in 2016 with the MLS platform MODISSA at the TUM city campus in Munich, Germany, is used to test our methodology. Each point in the dataset has 3D (X, Y, and Z) coordinates and an intensity value. A part of the test area has been manually labeled as ground truth, which includes the following eight categories: *artificial terrain*, *natural terrain*, *high vegetation*, *low vegetation*, *building*, *hardscape*, *artifact*, and *vehicle* (see Fig. 3). The dataset contains slightly more than 3M manually labeled points.

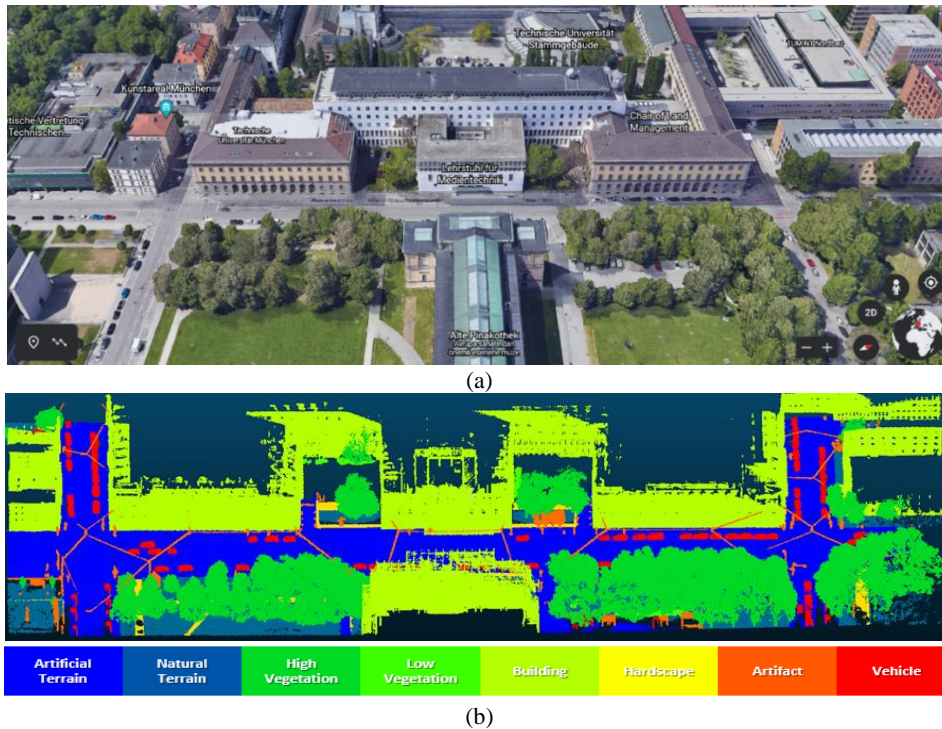


**Fig. 3.** TUM-MLS1 (a) real scene representation, and (b) point cloud with eight semantic labels (Zhu et al., 2020).

Toronto-3D, one of the publicly available point cloud datasets, was collected in 2020 from Avenue Road in Toronto, Canada (Tan et al., 2020). This dataset was separated into four sections, and consists of 78.3M points in total (see Fig. 4). Each point has 10 attributes, including point location (X,Y,Z), color information (RGB), intensity, GPS time, scan angle track, and label. The dataset covers the following eight object classes: *road*, *road marking* as pavement markings, *natural* as trees, *building*, *utility line* as power lines, *pole*, *car* and *fence* as vertical barriers. The L004 part of the dataset, which contains over 6.7M points, was utilized for this study. The unclassified points of the dataset were removed, and the road and natural classes were randomly subsampled to

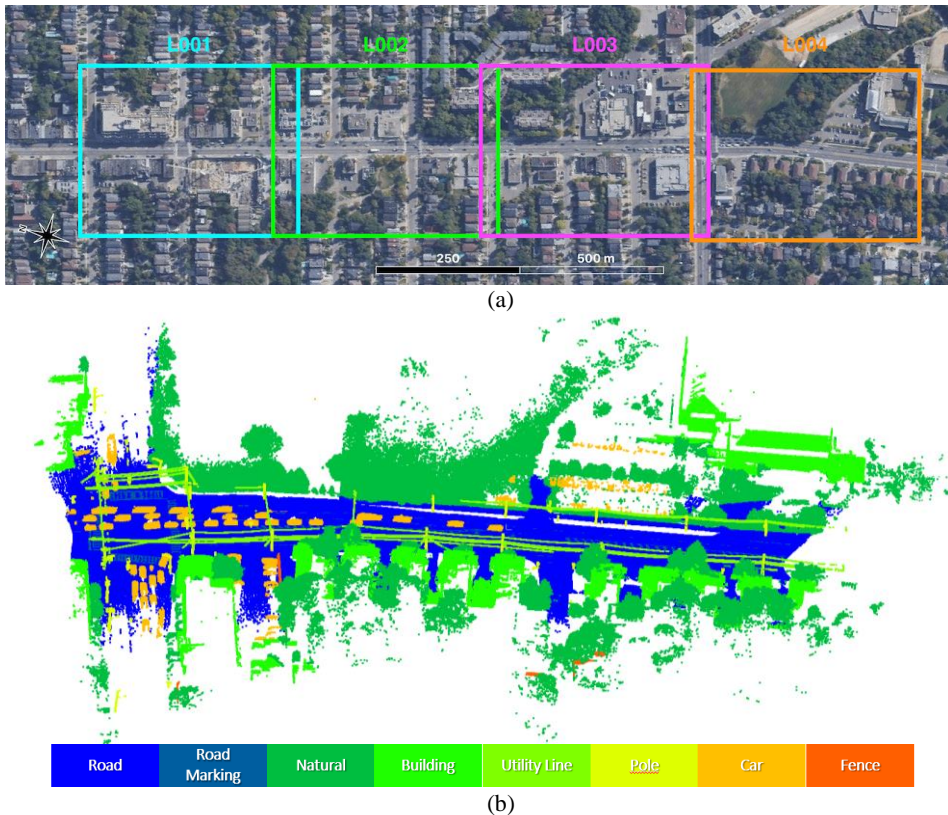


**Fig. 4.** Toronto-3D (a) real scene representation with four overlapped sections, and (b) point cloud with eight semantic labels (Tan et al., 2020).

1.8M and 1M respectively, to mitigate the imbalanced point number structure within the point cloud. The reduced point cloud contains a total of 3.94M labeled points.

In this study, both datasets are randomly divided into training (25%) and test (75%) sets using the holdout cross-validation technique, with the points reserved only for training are further divided into two groups randomly, training (80%) and validation (20%). The classification model is estimated with the training data, while the performance of the trained model is evaluated internally with the validation data. Finally, the test model is used to evaluate the classification results independently.

To investigate the effect of radius on classification, the radius parameter is tested using different values (i.e. 0.25m, 0.50m, and 0.75m), and the generated geometric features are fed into the RF classifier (with a fixed number of trees of 35). To extract the geometric features such as the normalized height (H), height difference ( $\Delta H$ ), the number of points (N) and the standard deviation of heights of points ( $\sigma H$ ) within the local neighborhood, the X, Y and Z coordinates of neighboring points are utilized. Also, how the point-based classification is affected by the features is tested on the 4 features described in Section 2. Besides, the relative importance of features is determined in MATLAB using the "Out of Bag Importance Estimates" of the RF algorithm used for classification. In addition, the correlation between features is one of the factors affecting

the result, so the strength of association between pairs of predictors can be inferred using predictor association estimation.

#### 4. Results and Discussion

Three radius parameters are assessed to understand how the size of the local cylindrical neighborhood affects the classification outcome. In this respect, Table 2 shows the differences between the classification performances of the testing set for with well-known user's accuracy, producer's accuracy, intersection over union (IoU), overall accuracy and kappa index measures of TUM-MLS1. When the radius is set to 0.25m, the classification accuracy computed with the geometric-based features obtained from the local cylindrical neighborhood is found to be the lowest. The best result, on the other hand, is obtained when a radius of 0.75m is chosen. Fig. 5 depicts the confusion matrix for the classification belonging to the best result (i.e. for radius 0.75m).

**Table 2.** Overall accuracy (O.A.) and kappa index (in %) of the TUM-MLS1 test data for all three different radius values tested ( $N_{0.25}$ : 0.25m ,  $N_{0.50}$ : 0.50m and  $N_{0.75}$ : 0.75m).

Class	$N_{0.25}$			$N_{0.50}$			$N_{0.75}$		
	User	Producer	IoU	User	Producer	IoU	User	Producer	IoU
<i>artificial terrain</i>	88.7	93.8	83.8	89.5	94.5	85.1	90.9	95.1	86.8
<i>natural terrain</i>	77.5	79.5	64.6	80.1	81.6	67.8	82.3	84.3	71.4
<i>high vegetation</i>	92.5	97.1	90.0	95.0	97.7	92.9	96.6	98.2	94.9
<i>low vegetation</i>	73.9	45.9	39.5	83.0	61.2	54.4	88.0	70.5	64.3
<i>building</i>	94.5	89.9	85.4	95.9	93.2	89.6	96.8	95.3	92.4
<i>hardscape</i>	70.1	47.7	39.6	78.6	55.2	48.0	82.8	59.0	52.6
<i>artifact</i>	82.7	59.7	53.1	87.6	71.8	65.2	89.6	77.6	71.2
<i>vehicle</i>	81.4	83.0	69.8	86.5	84.2	74.4	89.2	85.8	77.7
O.A.(%)	91.0			93.0			<b>94.5</b>		
Kappa(%)	87.1			90.0			<b>92.1</b>		

The classes *high vegetation* and *building* yield a successful performance, with accuracies over 95%, despite the confusion in these two classes. Because these classes dominate the dataset, they have an increasing influence on the final accuracy. The most common causes of classification errors are classes with similar properties, such as *artificial terrain* and *natural terrain*, overlapping objects (e.g., *high vegetation* vs. *artifact*), adjacent objects (*building* vs. *high vegetation*), and relatively small sampled classes (e.g. *low vegetation*, *hardscape* and *artifact*). Despite this, the overall accuracy and kappa are determined to be 94.5% and 92.1%, respectively. Considering the processing times, it was approximately 8 minutes, 14 minutes and 24 minutes for the case where the radii were 0.25m, 0.50m and 0.75m. Fig. 6 and Fig. 7 show whole test result and sample cases of the point-based classification with the RF classifier using the vertical cylindrical neighborhood with radius 0.75m.

		Classified Data								Row Total
		<i>artificial terrain</i>	<i>natural terrain</i>	<i>high vegetation</i>	<i>low vegetation</i>	<i>building</i>	<i>hardscape</i>	<i>artifact</i>	<i>vehicle</i>	
Reference Data	<i>artificial terrain</i>	<b>271008</b>	10672	2	29	1533	522	95	1070	284931
	<i>natural terrain</i>	19295	<b>133975</b>	80	141	2691	1166	497	1119	158964
	<i>high vegetation</i>	1	334	<b>871512</b>	200	14429	96	826	98	887496
	<i>low vegetation</i>	347	741	447	<b>7865</b>	798	147	457	358	11160
	<i>building</i>	3000	6647	26240	86	<b>769026</b>	362	987	949	807297
	<i>hardscape</i>	2332	5985	72	91	1420	<b>16049</b>	435	818	27202
	<i>artifact</i>	312	1642	3396	346	2705	431	<b>35637</b>	1472	45941
	<i>vehicle</i>	1905	2816	83	182	1602	600	819	<b>48497</b>	56504
	<i>Column Total</i>	298200	162812	901832	8940	794204	19373	39753	54381	<b>2279495</b>

Fig. 5. Confusion matrix of the TUM-MLS1 test data for radius 0.75m.

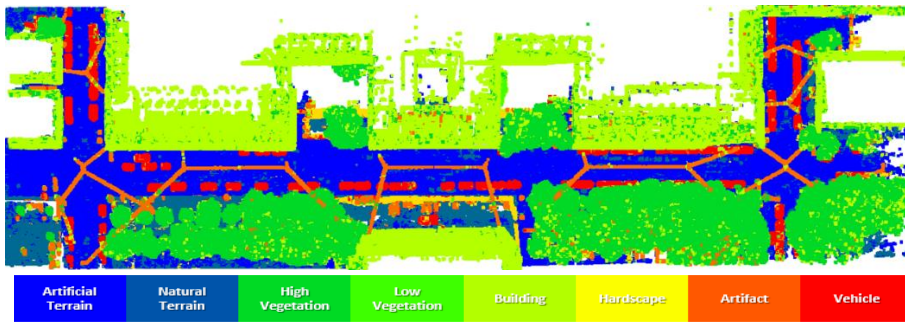


Fig. 6. Classified test set of TUM-MLS1 with radius 0.75m.

TUM-MLS1 dataset was classified by Sun et al. (2018) using 13 feature sets, including seven feature-based features (linear, spherical, full variance, anisotropy, feature entropy, and local curvature), two height features (mean height and height difference), three spatial features (normal vector), and one radiometric feature (intensity). In a way analogous to our study, the RF classifier was used and the number of trees was set to 200. Additionally, in contrast to our test set, 50% of the total dataset was used for training. When our findings are compared to the results provided by Sun et al. (2018), we observe a 2.4% improvement in overall accuracy and major improvements in the classes of *low vegetation* and *artifact* (see Table 3).

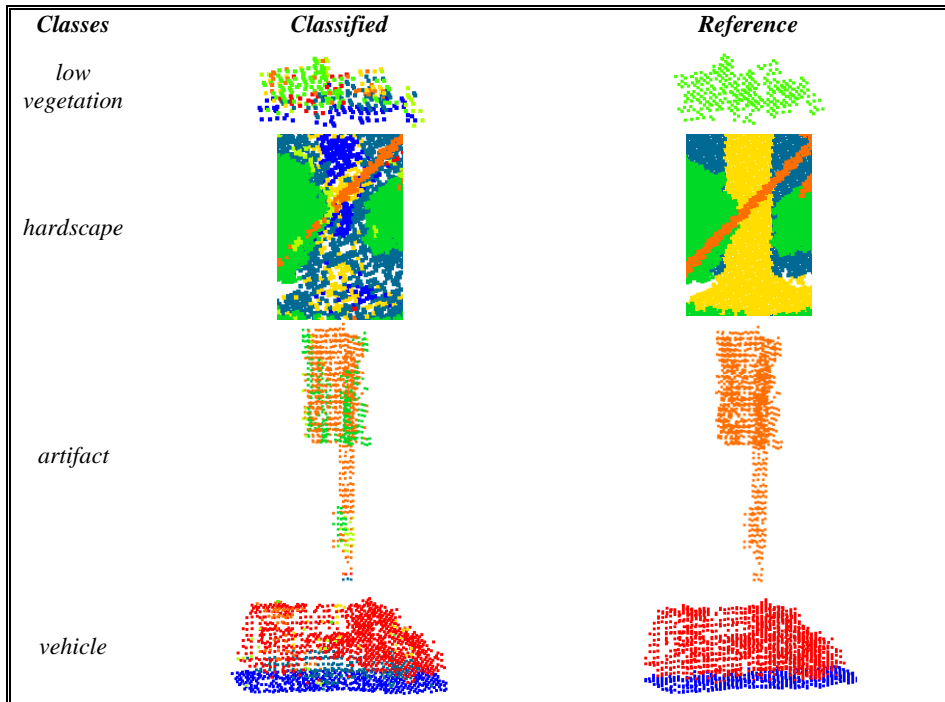


Fig. 7. Classes of TUM-MLS1's test dataset acquired with low accuracy (radius is 0.75m).

Table 3. Comparison to a state-of-the-art approach of TUM-MLS1. O.A. indicates the overall accuracy.

Class	Sun et al. (2018)		Our Approach	
	User	Producer	User	Producer
<i>artificial terrain</i>	<b>0.952</b>	0.943	0.909	<b>0.951</b>
<i>natural terrain</i>	<b>0.839</b>	<b>0.911</b>	0.823	0.843
<i>high vegetation</i>	0.931	0.972	<b>0.966</b>	<b>0.982</b>
<i>low vegetation</i>	0.787	0.496	<b>0.880</b>	<b>0.705</b>
<i>building</i>	0.933	0.931	<b>0.968</b>	<b>0.953</b>
<i>hardscape</i>	<b>0.844</b>	0.495	0.828	<b>0.590</b>
<i>artifact</i>	0.747	0.345	<b>0.896</b>	<b>0.776</b>
<i>vehicle</i>	0.827	0.848	<b>0.892</b>	<b>0.858</b>
O.A.	0.921		<b>0.945</b>	

Table 4 presents the classification performances of the Toronto-3D test data for the different radius sizes tested. The best result in overall accuracy was obtained when the radius was 0.75m as 94.5%, and the worst result was when the radius was 0.25m as 92.2%. As a result, we can conclude that the classification results obtained for Toronto-

3D and TUM-MLS1 are consistent. For Toronto-3D, the processing time increased to 65 minutes when the radius was 0.75m, whereas in all other cases it was completed in roughly the same amount of time as TUM-MLS1. Fig. 8 depicts the confusion matrix for the classification belonging to the best result (i.e. for radius 0.75m).

		Classified Data								Row Total
		road	road marking	natural	building	utility line	pole	car	fence	
Reference Data	road	<b>1316004</b>	26441	2386	560	0	76	4471	63	1350001
	road marking	62530	<b>142817</b>	19	5	0	0	282	0	205653
	natural	3983	7	<b>729133</b>	13334	1070	193	2168	112	750000
	building	1771	8	26607	<b>375283</b>	182	70	345	39	404305
	utility line	0	0	3783	459	<b>23234</b>	425	0	0	27901
	pole	147	3	1502	187	190	<b>51644</b>	33	0	53706
	car	4615	146	2952	257	0	63	<b>153083</b>	103	161219
	fence	110	0	489	64	0	0	159	<b>2604</b>	3426
	Column Total	1389160	169422	766871	390149	24676	52471	160541	2921	<b>2956211</b>

**Fig. 8.** Confusion matrix of the Toronto-3D test data for radius 0.75m

**Table 4.** Overall accuracy (O.A.) and kappa index (in %) of the Toronto-3D test data for all three different radius values tested. Bold ones indicate the best results. (N<sub>0.25</sub>: 0.25m , N<sub>0.50</sub>: 0.50m and N<sub>0.75</sub>: 0.75m)

Class	N <sub>0.25</sub>			N <sub>0.50</sub>			N <sub>0.75</sub>		
	User	Producer	IoU	User	Producer	IoU	User	Producer	IoU
road	94.3	97.7	92.2	94.4	97.8	92.4	94.7	97.5	92.5
road marking	87.0	68.9	62.5	86.3	67.7	61.1	84.3	69.4	61.5
natural	89.4	94.6	85.1	93.4	96.5	90.3	95.1	97.2	92.6
building	92.3	83.4	78.0	95.2	90.1	86.1	96.2	92.8	89.5
utility line	90.5	77.6	71.7	93.6	82.1	77.7	94.2	83.3	79.2
pole	97.6	89.0	87.1	98.3	94.2	92.7	98.4	96.2	94.7
car	91.5	90.7	83.6	94.7	93.5	88.9	95.4	95.0	90.8
fence	81.7	46.0	41.7	89.2	69.7	64.3	89.1	76.0	69.6
O.A.(%)	92.2			93.8			<b>94.5</b>		
Kappa(%)	88.7			91.1			<b>92.1</b>		

The high accuracy and prevalence of the classes *road*, *natural*, and *building* in the data had a significant impact on the classification result. One can observe a relatively strong confusion between the *road* and *road marking* classes. Although the overall classification accuracy is increased with increasing the radius parameter in our experiments, the best result for the *road marking* class is achieved when a small radius is set. It's possible that the color information in the dataset can help us distinguish between these two classes. As in TUM-MLS1, some confusion has also been observed between classes that are very close and overlapped, such as *natural*, *building*, and *utility line*. Due to the greater number of samples compared to the TUM-MLS1 dataset, the class *car* in Toronto-3D dataset is identified with an accuracy of over 90 percent. The classified outputs of Toronto-3D dataset for radius 0.75m are illustrated in Fig. 9 and Fig.10.

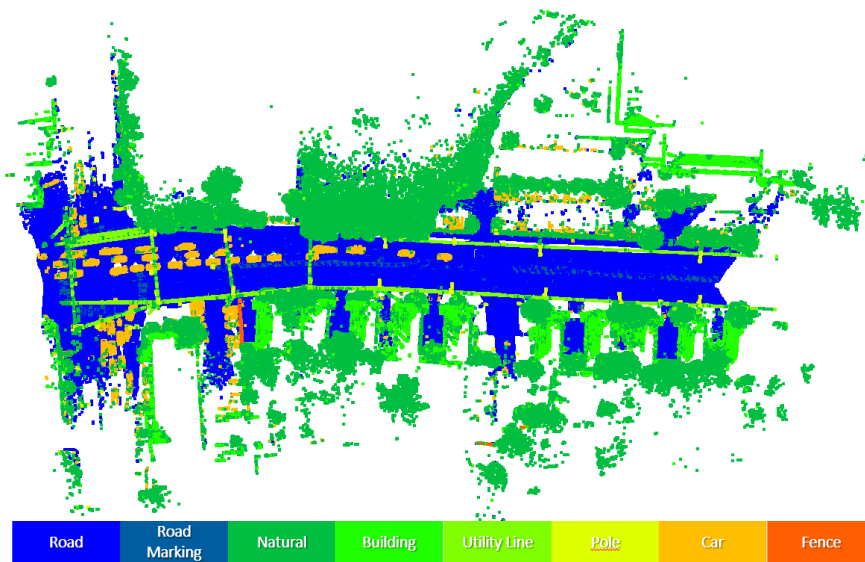


**Fig. 9.** Classification results of Toronto-3D with radius 0.75m.

The results of the feature importance test indicate that normalized height is the most significant predictor of the four predictors for TUM-MLS1. Therefore, precise terrain elevation estimation at each point is essential. The most significant parameter for Toronto-3D is the number of neighborhood points. Scale determination is crucial because this parameter is highly dependent on the point density in the point cloud and the size of the neighborhood. According to the results of the tests, there is almost no correlation between the features utilized (see in Fig. 11).

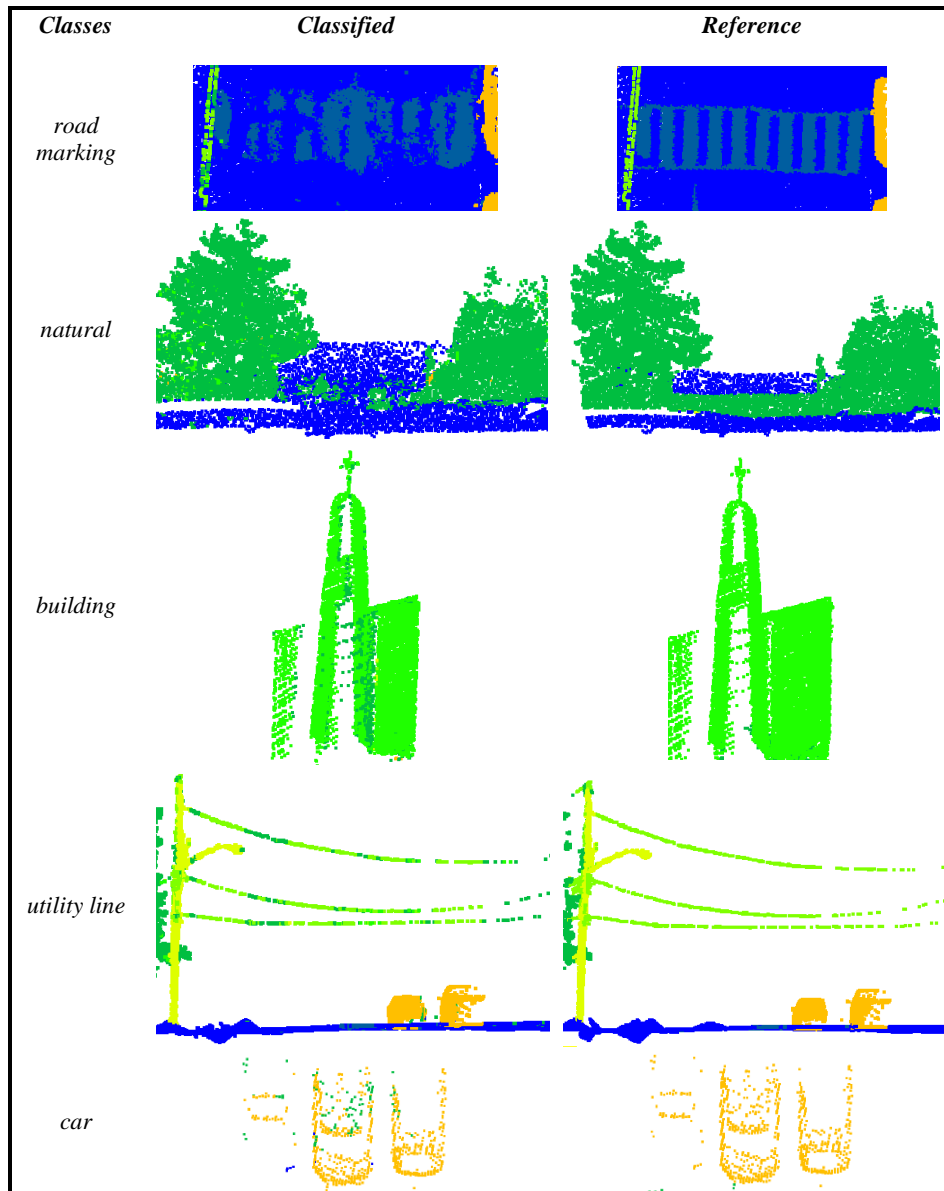


**Fig. 10.** Classes of Toronto-3D's test dataset with radius 0.75m.

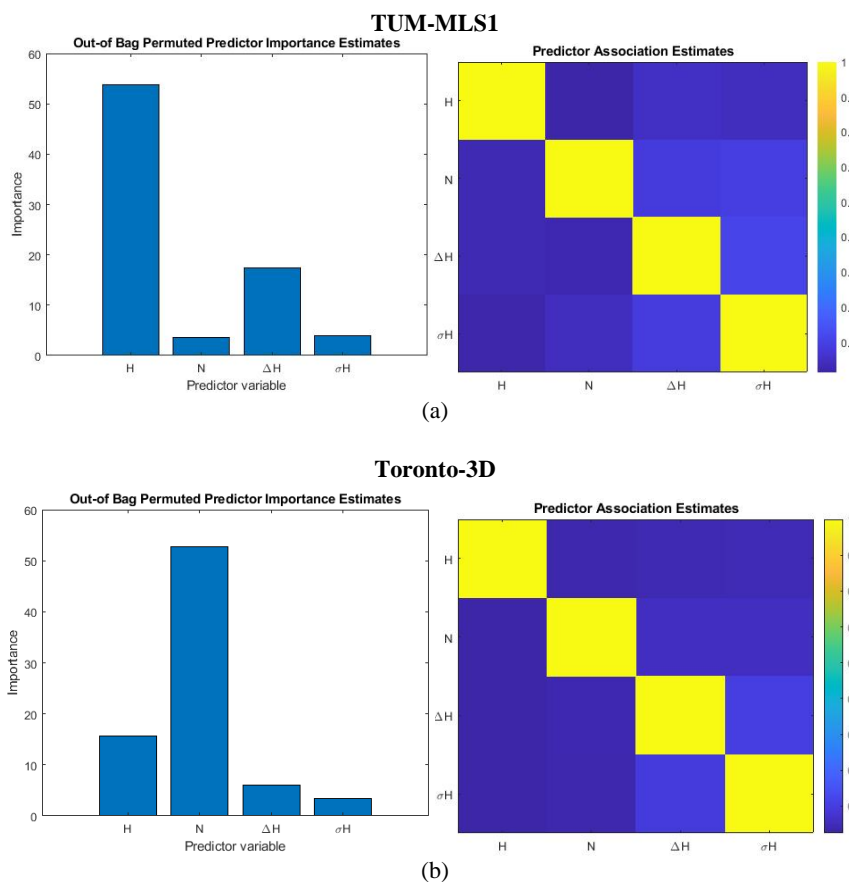


**Fig. 11.** Importance of features estimated via Out of Bag Importance Estimates of the RF algorithm and Predictor Association Estimates for (a) TUM-MLS1, and (b) Toronto-3D.

## 5. Conclusion

The original features of dense point cloud data acquired using mobile laser scanners are weak in the absence of color information. Therefore, in this study, a neighborhood relationship between the points in the point cloud was formed using the cylindrical neighborhood type. Thereafter, features are extracted based on their proximity to each other in order to improve classification performance.

Overall accuracies of over 90% can be obtained by utilizing four geometric features via the cylindrical neighborhood relationship. Classification errors are most frequently caused by classes with similar properties, such as *artificial* and *natural terrain* of TUM-MLS1 dataset, and *road* and *road marking* of Toronto-3D dataset, overlapping objects (e.g., *high vegetation* vs. *artifact* of TUM-MLS1, and *natural* vs. *car* of Toronto-3D), adjacent objects (*building* vs. *high vegetation*), and classes with a small sample size (e.g. *low vegetation*, *hardscape* and *artifact*). Indeed, the results for specific classes (*low vegetation*, *hardscape*, and *artifact*) are computed to be relatively low and, in general, cannot reach a satisfactory level. Nevertheless, the cylindrical neighborhood's major

drawback appears to be its processing time, which is significantly longer than that of its counterparts, such as the k-nearest neighbor or spherical neighborhood. Given that the processing load increases with increasing data density, various approaches (segmentation, voxel, etc.) can be used to improve the processing of large datasets and reduce the processing load. It is worth noting that the sample size of the classes may have an effect on the classification result. Fixed radius selection may not be appropriate for classes with a small sample size, depending on the cloud point density.

Our future research will also examine classification strategies for MLS, including deep learning. The introduced strategy will be tested on other benchmark datasets publicly available. Moreover, the feature set will be augmented with other features, and feature importance will be emphasized by the classifier-independent feature selection methods.

## Acknowledgements

The authors would like to thank Dr. Marcus Hebel, Joachim Gehring and Weikai Tan for providing the datasets. The TUM-MLS1 dataset is copyrighted by Fraunhofer IOSB and it is made available under the CC BY-NC-SA 4.0 License. Toronto-3D dataset belongs to Mobile Sensing and Geodata Science Lab, University of Waterloo. Toronto-3D is distributed under the CC BY-NC 4.0 License.

## References

- Atik, M. E., Duran, Z., Seker D. Z. (2021). Machine learning-based supervised classification of point clouds using multiscale geometric features, *ISPRS International Journal of Geo-Information* **10**(3), 187.
- Bentley, J. L. (1975). Multidimensional binary search trees used for associative searching, *Communications of the ACM* **18**, 509–517.
- Breiman, L. (2001). Random Forests, *Machine Learning* **45**, 5–32.
- Brodu, N., Lague, D. (2012). 3D terrestrial lidar data classification of complex natural scenes using a multi-scale dimensionality criterion: Applications in geomorphology, *ISPRS Journal of Photogrammetry and Remote Sensing* **68**, 121–134.
- Demantké, J., Mallet, C., David, N., Vallet, B., (2012). Dimensionality based scale selection in 3d lidar point clouds, *The International Archives of the Photogrammetry, Remote Sensing and Spatial Information Sciences* **38**, 97–102.
- Filin, S., Pfeifer, N. (2005). Neighborhood systems for airborne laser data, *Photogrammetric Engineering & Remote Sensing* **71**(6), 743–755.
- Gao, H., Cheng, B., Wang, J., Li, K., Zhao, J., Li, D. (2018). Object classification using CNN-based fusion of vision and LiDAR in autonomous vehicle environment, *IEEE Transactions on Industrial Informatics* **14**, 4224–4231.
- Guan, H., Li, J., Cao, S., Yu, Y. (2016). Use of mobile LiDAR in road information inventory: a review, *International Journal of Image and Data Fusion* **7**, 219–242.
- Guo, Z., Feng, C. C. (2018). Using multi-scale and hierarchical deep convolutional features for 3D semantic classification of TLS point clouds, *International Journal of Geographical Information Science* **34**, 661–680.
- Günen, M.A. (2022). Adaptive neighborhood size and effective geometric features selection for 3D scattered point cloud classification, *Applied Soft Computing* **115**, 108196.
- Kukko, A., Kaartinen, H., Hyypä, J., Chen, Y. (2012). Multiplatform mobile laser scanning: usability and performance, *Sensors* **12**, 11712–11733.
- Lou, Y., Zhang, T., Tang, J., Song, W., Zhang, Y., Chen, L. (2018). A fast algorithm for rail extraction using mobile laser scanning data, *Remote Sensing* **10**, 1998.

- Sun, Z., Xu, Y., Hoegner, L., Stilla, U. (2018). Classification of MLS point clouds in urban scenes using detrended geometric features from supervoxel-based local contexts, *ISPRS Annals of the Photogrammetry, Remote Sensing and Spatial Information Sciences* **4**, 271–278.
- Tan, W., Qin, N., Ma, L., Li, Y., Du, J., Cai, G., Yang, K., Li, J. (2020). Toronto-3D: A large-scale Mobile LiDAR dataset for semantic segmentation of urban roadways, *2020 IEEE/CVF Conference on Computer Vision and Pattern Recognition Workshops (CVPRW)*. Seattle, WA, USA, 797–806.
- Thomas, H., Goulette, F., Deschaud, J.-E., Marcotegui, B., LeGall, Y. (2018). Semantic classification of 3D point clouds with multiscale spherical neighborhoods, *International Conference on 3D Vision (3DV)*, Verona, 390–398.
- Vaaja, M., Kukko, A., Kaartinen, H., Kurkela, M., Kasvi, E., Flener, C., Hyypä, H., Hyypä, J., Järvelä, J., Alho, P. (2013). Data processing and quality evaluation of a boat-based mobile laser scanning system, *Sensors* **13**, 12497–12515.
- Wang, Y., Chen, Q., Liu, L., Li, X., Sangaiah, A. K., Li, K. (2018). Systematic comparison of power line classification methods from ALS and MLS point cloud data, *Remote Sensing* **10**, 1222.
- Weinmann, M. (2015). Semantic point cloud interpretation based on optimal neighborhoods, relevant features and efficient classifiers, *ISPRS Journal of Photogrammetry and Remote Sensing* **105**, 286-304.
- Weinmann, M., Jutzi, B., Mallet, C. (2013). Feature relevance assessment for the semantic interpretation of 3D point cloud data, *ISPRS Annals of the Photogrammetry, Remote Sensing and Spatial Information Sciences* **II-5/W2**, 313–318.
- Zhang, W., Qi, J., Wan, P., Wang, H., Xie, D., Wang, X., Yan, G. (2016). An easy-to-use airborne LiDAR data filtering method based on cloth simulation, *Remote Sensing* **8**, 501.
- Zheng, M., Lemmens, M., van Oosterom, P. (2017). Classification of mobile laser scanning point clouds from height features, *The International Archives of the Photogrammetry, Remote Sensing and Spatial Information Sciences* **42**, 321–325.
- Zhu, J., Gehring, J., Huang, R., Borgmann, B., Sun, Z., Hoegner, L., Hebel, M., Xu, Y., Stilla, U. (2020). TUM-MLS-2016: An annotated mobile lidar dataset of the TUM city campus for semantic point cloud interpretation in urban areas, *Remote Sensing* **12**, 1875.